

# Investigation of Cholera Toxin Interaction Mechanism for Structure-Based Drug Design

Ayhan Ünlü<sup>1</sup> 

<sup>1</sup>Trakya University Medical Faculty,  
Department of Biophysics, Edirne,  
Turkey

Ayhan ÜNLÜ

## ABSTRACT

Cholera is a disease that is developed by parasitizing the bacteria called vibrio cholera in the small intestine of people and it causes severe watery diarrhea, if it is left untreated, it can result in death. The bacteria is transmitted to the people through the digestive tract with water and nutrients, starting with vomiting and going on with severe diarrhea. A potent enterotoxin, Cholera Toxin (CT) which is secreted by vibrio cholera is largely responsible for the disease. It first emerged in India and began to spread to the world between 1827-1975. The cause of the disease, Vibrio cholerae bacteria, which has been known since ancient times with high outbreaks and high mortality rates, has less resistance to external influences and dies in 10-15 minutes at 55°C and in 1-2 minutes at boiling temperature. They are not able to resist dryness, sunlight and acids. Gastric acidity inactivates the vibrations in a short time, which protects many people from being caught in cholera. ADP-Ribosylating Toxins (ADPRT), also including cholera toxin synthesized by this bacteria, are a large and potentially fatal toxin family. They are secreted by pathogenic bacteria and inhibit the functions of human target proteins. Based on structure-based multiple sequence alignments, the ADPRT family is classified into two groups according to the Nicotinamide Adenine Dinucleotide (NAD) that binds Diphtheria Toxin (DT) and CT. DT group toxins change eukaryotic elongation factor 2 and disrupt protein synthesis in eukaryotic cells. DT, exotoxin A (ETA) and cholix toxin are among the members of this group. CT group toxins target various essential proteins in host organisms. For example, CT and temperature-varying enterotoxin target Arg on Gs-R on G protein. This leads to uncontrolled adenylate cyclase activity. Although ADPRT enzymes exhibit a variety of functions and low sequence identities, they share common structural and functional characteristics. This toxin family has the ability to catalyze NAD by using the same pathway with poly ADP-ribose polymerases. We think that being clarified as a matter of the cholera toxin structure, which is the member of this family, will play an important role in the development of many drug design studies such as being able to interfere in significant proteins structure for cancer cells and the development of various catalysis mechanisms. In this study, we investigated the three-dimensional structure of cholera toxin, which is an important member of the ADPRT family, and the interface which will interact with the other amino acids whose binding energies are higher than other amino acids which are situated in the structure (hot spot) by using theoretical and experimental methods. As a result of our theoretical and experimental studies we think that the 12 amino acid sequence of Cholera toxin, constituting the common structural region that binds to NAD in the ADP-ribosylating toxins family is the sequence of 61- STSISLRSALHLV-72.

**Keywords:** Cholera Toxin, ADP-ribosylating toxins, poly ADP-ribose polymerases, nicotinamide adenine dinucleotide (NAD), protein-ligand interaction

## Yapı Bazlı İlaç Tasarımı İçin Kolera Toksin Etkileşim Mekanizmasının İncelenmesi

### ÖZET

Kolera, vibrio kolera adı verilen bakterilerin insanların ince bağırsağında konaklamasıyla gelişen ve şiddetli sulu ishale neden olan ve tedavi edilmediğinde ölüme sonuçlanabilen bir hastalıktır. Bakteriler su ve besinlerle, sindirim yolu aracılığıyla insanlara bulaşır ve hastalık kusma ile başlayıp şiddetli ishale devam eder. Hastalıktan büyük ölçüde sorumlu olan Kolera Toksini (CT), vibrio kolera tarafından salgılanan güçlü bir enterotoksindir. Hastalık ilk olarak Hindistan'da ortaya çıkmış ve 1827-1975 yılları arasında dünyaya yayılmaya başlamıştır. Hastalığın nedeni olan Vibrio Kolera bakterisi eski zamanlardan beri salgınlara ve yüksek ölüm oranlarına sebep olarak bilinmektedir. Bakteri dış etkenlere karşı dirençsizdir ve 55°C'de 10-15 dakikada, kaynama sıcaklığında 1-2 dakikada ölür. Kuru ortamlar, güneş ışığı ve asite direnemezler. Mide asiti titreşimleri kısa sürede etkisiz hale getirir. Böylece çoğu insan kolera yakalanmaktan korunur. CT, ADP-Ribozilleyen Toksinler (ADPRT) ailesine dahildir. Bu toksin ailesi geniş ve potansiyel olarak ölümcül toksinlerdir. Patojenik bakteriler tarafından salgılanırlar ve insan hedef proteinlerinin fonsiyonlarını inhibe ederler. ADPRT ailesi, difteri toksini (DT) ve kolera toksinini (CT) bağlayan NAD'a (Nikotin Amid Dinükleotot) göre iki gruba ayrılır. DT grubu toksinler elengasyon faktörü 2'yi değiştirir ve ökaryotik hücrelerde protein sentezini bozar. DT, ekzotoksin A (ETA) ve cholix toksin bu grubun üyeleri arasındadır. CT grubu toksinleri, konakçı organizmadaki çeşitli temel proteinleri hedefler. Örneğin CT ve sıcaklıkla değişen enterotoksin, G proteininde Gs-R üzerindeki Arg'yi hedefler. Bu, kontrolsüz adenilat siklaz aktivitesine yol açar. ADPRT enzimleri çeşitli işlevler ve düşük dizi benzerlikleri göstermelerine rağmen, ortak yapısal ve işlevsel özellikler gösterirler. Bu toksin ailesi, ADP-riboz polimerazlarla aynı yolu kullanarak NAD'ı katalize etme yeteneğine sahiptir. Bu ailenin bir üyesi olan kolera toksin yapısının aydınlatılmasının, kanser hücreleri için önemli olan protein yapılarına müdahale edilebilmesi ve çeşitli kataliz mekanizmalarının geliştirilmesi gibi birçok ilaç tasarımı çalışmasının geliştirilmesinde önemli rol oynayacağını düşünmekteyiz. Bu çalışmada, ADPRT ailesinin önemli bir üyesi olan kolera toksininin üç boyutlu yapısını ve bağlanma enerjileri, yapıda bulunan diğer aminoasitlerden yüksek olan aminoasitlerle etkileşime girecek arayüzünü, deneysel ve kuramsal yöntemler kullanılarak araştırdık. Teorik ve deneysel çalışmalarımız sonucunda, ADP ribozilleyen toksinler ailesinde NAD'a bağlanan ortak yapısal bölgeyi oluşturan Kolera toksininin 12 aminoasitlik dizisinin 61- STSISLRSALHLV-72 olduğunu düşünüyoruz.

**Anahtar Sözcükler:** Kolera Toksini, ADP-ribozilleyen toksinler, ADP-Ribozil Polimerazlar, Nikotin adenin Dinükleotit, Protein-Ligand etkileşimi

**Correspondence:** Ayhan Ünlü  
Trakya University Medical Faculty, Department  
of Biophysics, Edirne, Turkey  
**Phone:** +902842357641  
**E-mail:** ayhan@trakya.edu.tr

**Received:** 24 February 2022

**Accepted:** 1 March 2022

The Italian Filippo Pacini first identified cholera toxin (CT), produced by *Vibrio Cholerae* (VC), as the cause of cholera in 1854 (1), and Robert Koch rediscovered it nearly 30 years later (2). He postulated the existence of CT in 1886, claiming that the symptoms induced by *Vibrio cholerae* which is caused by a toxin generated by the bacterium. S. N. De in Calcutta in 1959 verified this insightful hypothesis, demonstrating that cell-free extracts from VC cultures could produce excess fluid in rabbits when injected into ligated small intestine loops (3). In the same year, NK Dutta and colleagues at the Haffkine Institute in Bombay, India, revealed that a crude protein extracted from the culture filtrate of *V. cholerae* causes diarrhea in newborn rabbits (4), confirming De's findings. De's discovery of the cholera toxin and its exotoxin nature laid the groundwork for present cholera study into the disease's molecular basis. Richard Finkelstein's group was able to isolate and purify the CT (5,6). Using gel filtration chromatography and membrane ultrafiltration, his team isolated the active ingredient from *V. cholerae* culture supernatants and named it "cholera toxin." SDS-polyacrylamide gel electrophoresis, which dissociates and separates non-covalently bound protein components, revealed two distinct kinds of subunits in cholera toxin. The terms "cholera toxin" and "cholera toxinogenoid" were distinguished. The latter was a protein with a molecular weight of about 56,000 Da that generated spontaneously from the dissociation of cholera toxin and was named cholera toxinogenoid. It was antigenically similar to the original toxin, however it lacked the toxin's harmful properties. The B-subunit pentamer was later X-ray crystallography at 2.5 Å resolution was used to solve and improve the three-dimensional structure of hexameric AB<sub>5</sub> CT (7). This structure is similar to that of *Escherichia coli* heat-labile enterotoxin, with which cholera toxin has 80 percent sequence homology. The poisonous A-subunit is found embedded in the symmetrical pentameric pore-like structure produced by five B-subunits, according to X-ray crystallographic investigations (8). Despite being generated as a single polypeptide chain, the mature A-subunit (240 aa) is eventually separated into two sections: a wedge-shaped A1 domain and an elongated A2 domain with an alpha helical structure and a tail that extends through the pore formed by the B-pentamer discovered as harmless and immunogenic. Finkelstein's team was able to crystallize cholera toxinogenoid, then recombine them to make active toxin (9). The active principle "cholera toxin," which is toxic in nature and is known as A-subunit, as well as the nontoxic B-pentameric "cholera toxinogenoid," both played a role in eliciting cholera symptoms. Biochemical studies later revealed that CT's heterogeneous subunit structure consists of one A-subunit linked to five B-subunits.

### The Structure of CT

Cholera toxin is a member of the AB<sub>5</sub> bacterial toxin family (10), so named because of its unique architecture, which consists of a catalytically active A-subunit and a nontoxic pentameric B-subunit (B<sub>5</sub>) (Figure 1). CT is a heterogeneous protein made up of two types of subunits (11): a large one with an estimated molecular weight (MW) of approximately 28 kDa and several small ones with estimated MWs of 8–10 kDa each and an aggregate size of ca 56 kDa.

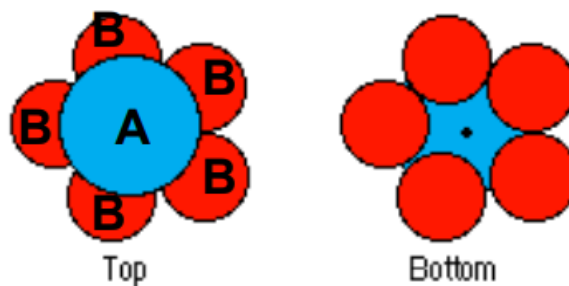


Figure 1: A and B subunit of Cholera Toxin

A-subunit has a length of 258 amino acids (aa). The signal peptide (1–18 aa), A1 chain (19–212 aa), and A2 chain (213–258 aa) are all included. The hazardous enzymatic activity is caused by the A1 chain, also known as CT alpha chain or NAD diphthamide adenosine diphosphate (ADP)-ribosyl transferase. Cholera enterotoxin gamma chain is another name for the A2 chain (12). A disulfide bridge between cysteines at locations 205 and 217 aa connects the two chains A1 and A2. Protein ADP-ribosylation domain is found in the A1 subunit. The monomer of the B-subunit is 124 amino acids long. A signal peptide (1–21 aa) and a mature B chain (22–124 aa) make up this segment. A pentameric ring is formed by the assembly of five B-subunits (13) (Figure 2).

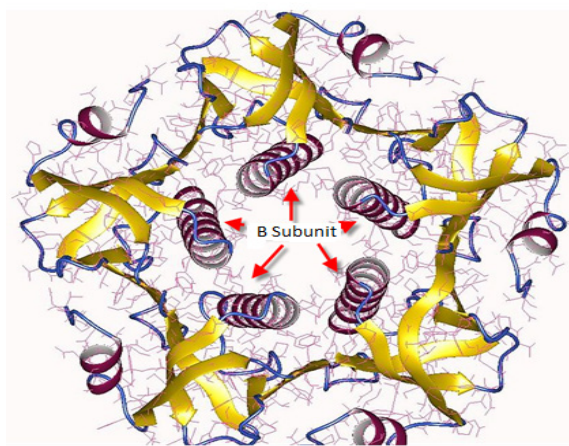


Figure 2: Secondary Structure of CT

A-subunit's secondary structure is made up of a combination of alpha-helix, beta-sheet, and random coil structural components. The alternative alpha and beta chains make up the majority of the A1 chain (19–212 aa), whereas the alpha-helical structure makes up the majority of the A2 chain. The amino acid residues are distributed among just two alpha-helices in the secondary structure of the CT B-subunit (14), with the remaining beta-strands enabling its membrane attachment feature. It consists of a single disulfide bridge between cysteines at 30 and 107 aa residues.

X-ray crystallography at 2.5 Å resolution was used to solve and improve the three-dimensional structure of hexameric AB5 cholera toxin (6). This structure is similar to that of *Escherichia coli* heat-labile enterotoxin, with which cholera toxin has 80 percent sequence homology. The poisonous A-subunit is found embedded in the symmetrical pentameric pore-like structure produced by five B-subunits, according to X-ray crystallographic investigations. Despite being generated as a single polypeptide chain, the mature A-subunit is eventually separated into two parts: a wedge-shaped A1 domain and an elongated A2 domain with an alpha helical structure and a tail that extends through the pore formed by the B-pentamer.

At least 20 hydrogen bonds and inter-subunit salt bridges stabilize the B-pentamer, with 10 of them located in the central pore. Furthermore, hydrophobic groups bind tightly at the subunit interface, generating significant packing of subunits against one another. This gives B-subunits in the intestinal environment a lot of stability when it comes to bile, proteases, and other things. The inner surface of the ring of B-subunits is hydrophobic, and a number of positive and negative charges line the central wall.

The pentamer's monomers form a six-stranded antiparallel  $\beta$ -sheet with a sheet from the next subunit, giving the ring a smooth outer surface, and lengthy-helices form a helical barrel in the core. During the creation of their structure, these helices softly bend inward, lowering the effective diameter of the pore from 16 Å (amino terminus) to 11 Å (carboxyl terminal).

The A2 domain and the B-pentamer are involved in the non-covalent interactions between the A and B subunits. The A-A1 subunit's and A2 domains are connected by an exposed loop with a proteolytic cleavage site (after arginine 192) and a disulfide bond that spans the cleavage

site. The enzymatically active A1 peptide is generated by proteolytic cleavage within the exposed loop of the A-subunit, which is responsible for hazardous action. The scaffolding that holds the A- and B-subunits together is formed by the A2 chain. The remaining four amino acids at the COOH-terminal of A2, lysine-aspartate-glutamate leucine or KDEL, emerge from the associated toxin molecule and are not involved in interactions with the pentameric B-subunit.

In this study for theoretical studies, a template file of Cholera toxin which is registered in the protein data bank with the code 2A5F was used, and also for experimental studies, lyophilized powder toxin which is known as sigma-C8052 obtained from *Vibrio Cholera* was used in the study.

## MATERIALS AND METHODS

### *Molecular dynamics (MD) simulations*

We were able to achieve the optimum model by combining the docking process with MD simulation to optimize the protein interface structure. Nonetheless, explicit constraint functions were not applied to retain the original docking connections during the simulation. Using the Kollman all-atom force field, the energy was initially reduced using 1000 steps of steepest descents and conjugate gradient was minimized in 2000 steps for structures. The unbounded cutoff and dielectric constant were set at 1 and 8 Å, respectively, and the dielectric function was distance dependent. Energy minimization with a classical force field was used to reduce unrealistically close steric clashes and substantial deviations that emerge from perfect geometry of conformational changes of amino acid side chains following docking. The energy-minimized structure was used as the starting point for the MD simulation. All MD simulations were performed using the NAMD (Not (just) Another Molecular Dynamics program) molecular simulation tool. The interactions between CT and NAD version 2.9 were examined using molecular dynamics (MD) simulations at 300 K and pH 7.0. A parallel molecular dynamics algorithm named NAMD was created to achieve high-performance simulation of massive biomolecular systems. NAMD has a number of advantages, including the ability to run on single desktop and laptop computers, as well as the ability to expand to hundreds of processors on high-end parallel platforms and tens of processors on low-cost commodity clusters. MD simulation was utilized to identify particular interactions at the interface, compute inter-residue lengths, and other computations, and the final structure was produced.

### Molecular docking

By using Autodock, the collected data of modeled structures (pdb-format) from DataBank were combined with supplemental data for cholera toxin. For genetics modeling, Lamarck's mechanism was applied, which is the notion of acquired traits being transmitted down from one generation to the next. The protein was given Kollman united atom charges (15), solvation parameters, and polar hydrogen, and Autodock employed Gastegier charges. The default distance between grid points was set at 0.375. Grid boxes' x, y, and z axes were set to 480, 260, and 280, respectively. These dimensions included all of CT's amino acid residues as well as grid sizes big enough to include all of CT's domains. The initial goal was to decode the binding domain. The step size was 0.2, and 50 simulation runs were completed. The torsion and orientation angles were both 50 degrees. 1000.0 for grid energy, 0.5 for cluster tolerance, 0.8 for crossover rate, 0.02 for mutation rate, 1 for maximum number of top individuals, and 1000 for maximum number of generations are the other adjusted data values.

### Obtaining the subunits of Cholera toxin by Trypsin Partial Digestion

CT was partly digested for 60 minutes at 37 degrees Celsius in the presence of 50 mM Tris-HCl with trypsin (molar ratio 1/200), 250 mM sucrose, 7 mM MET, and 0.2 mM PMSF at pH 7.4. To inhibit the process, a 1:1 ratio of soybean meal-derived trypsin inhibitor was added, then denatured with SDS. Electrophoresis (SDS-PAGE) and chromatographic techniques were used to purify trypsin-separated fractions. Protein concentration spin columns were used to concentrate the samples (Vivaspin-10.000). ELISA was used to assess the level of ADP-ribosylation activity in the samples.

### Chromatography Analysis

The study employed a HiPrep Sephacryl S-100 (16 x 60 cm) column for filtration chromatography. The column's total volume ( $V_c$ ) was determined to be 120 ml, with a dead volume ( $V_0$ ) of 40 ml. Aprotinin (6,5 kDa), carbonic anhydrase (29 kDa), ovalbumin (43 kDa), BSA (66 kDa), and conalbumin (75 kDa) standards were used to calibrate the column, and gel-phase distribution coefficients ( $\mu$ ) were determined and a calibration graph was constructed based on the arrival volume. Mobility was calculated using the following formula:

$$\mu = \frac{V_e - V_0}{V_c - V_0}$$

The protein samples were divided into fragments, and the arrival volumes of these pieces were determined using the calibration graph. The samples' optical densities were evaluated at 280 nm, 0.35 mPa pressure, 0.8 ml/min velocity, and 0.5 ml after separation.

### Electrophoresis Analysis

The Laemmli technique (16) was used to evaluate the samples using sodium dodecyl sulfate polyacrylamide gel electrophoresis (SDS-PAGE). To create a 12 percent separation gel, a silicon separator was placed between the glass plates. To obtain a smooth gel surface, a 1 cm water layer was produced and allowed to polymerize for 30 minutes. After pouring the water layer on the gelatin, a 5% healing gel was applied. The comb was expected to polymerize when it was put between glass platens to form wells for loading samples. The samples were boiled for 2 minutes after being combined with a denaturing buffer at a 1:1 ratio. Run-off buffer was added to the electrophoresis tank. During sample loading, a multi-protein standard (Fermentas Protein Ladder) with molecular weights ranging from 10 to 260 kDa was used as a molecular weight standard in a well. The current cutoff occurred when the labeling dye had reached the end of the gel. The gel was removed from the glasses and coomassie brilliant blue was used to stain them. The excess dye was then removed from the gel using a mixture of 7% acetic acid and 30% methanol. The gel, which had been dyed with protein bands, was put on 3 mm Whatman filter paper, covered with stretch film, and dried in a gel drier under vacuum for an hour at 80 °C.

### Thermal Shift Assay

Heat Shift Assay is a real-time PCR assay that detects thermal denaturation of proteins in the presence of a fluorescent dye (SYPRO orange). The intensity of fluorescent light is displayed as a function of temperature, forming a sigmoidal curve characterized by a two-state transition. The Boltzmann equation was used to calculate the transition curve's turning point ( $T_m$ ). A PCR equipment and a related "96 well plate" were utilized for the analysis. For each sample, the experiment was carried out three times. PARPs were applied in increasing quantities to the PARPs applied groups prior to the addition of SYPRO Orange. The fluorescence intensity was measured between 15 °C and 90 °C with an interval of 0.5 °C at 450-490 nm excitation and 560-580 nm detection throughout a 10 second time period (0.5 °C / 15 sec).

## RESULT AND DISCUSSION

Although A fraction of this enterotoxin synthesized by *Vibrio cholerae* is a single molecule, B fraction is in the form of 5 molecules. After the B component of the toxin binds to the surface of intestinal epithelial cells, the A sub-section enters the cytoplasm and decomposes there. This fraction disrupts the function of the regulatory protein that controls the activity of the enzyme adenylate cyclase in cells and makes it ineffective, so that adenylate cyclase shows continuous activity. This over-synthesized substance causes ATP to turn into cyclic AMP (cAMP) in excess. In cAMP this substance causes excess fluid and electrolyte to pass through the intestinal epithelial cells into the lumen. Since a significant part of the fluid comes from the blood, it causes the bicarbonate to come out of the blood together with the fluid and the pH of the blood to decrease, and accordingly it leads to the formation of acidosis, which initiates a process that becomes a problem for the host cells.

In our study, in order to understand the structure of CT, the crystal images of the three-dimensional structure of the toxin were displayed in the PyMol program and the regions where it interacted were analyzed (Figure 3). Our study was completed on the TR-Data Grid National Information Network, available for researchers within TUBITAK, by performing molecular dynamics calculations such as exact determination of attachment points on the CT, flexibility calculations, and various simulation studies.

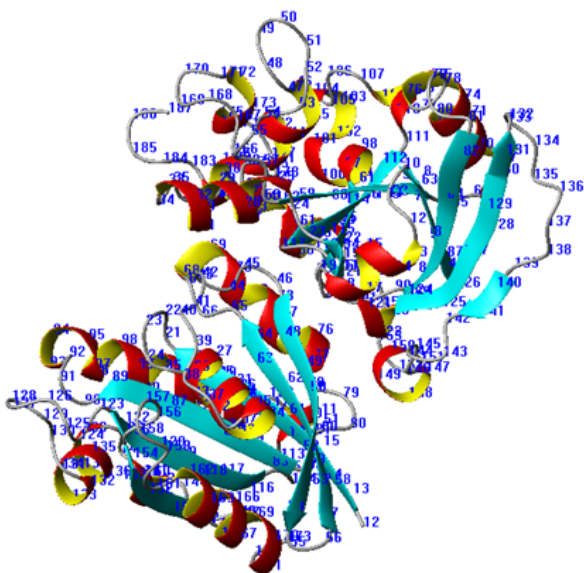


Figure 3: Secondary Structure of Cholera Toxin

The determined structure of cholera toxin was simulated with water molecules at 300°K to determine its most probable conformation (Figure 4)

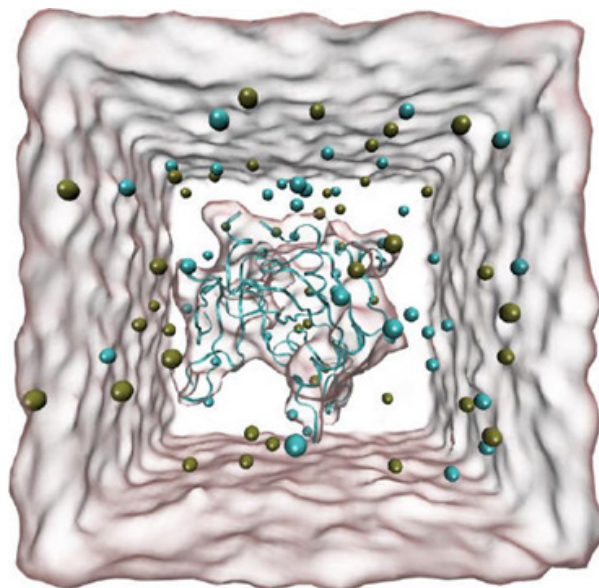


Figure 4: Cholera Toxin Simulation Study

During these processes the required regions were ordered from smallest to largest according to the calculated energies of the most likely interaction regions by subtracting similarity scores with a set of structural and geometric alignment algorithms. In the theoretical calculations, bond flexibility, bending angles, dihedral angles, interactions of amino acids with H atoms in the liquid medium where amino acids exist, Van der Waals interactions between atoms that make up amino acids, and electrostatic interactions arising from the charges of atoms were taken into account.

Cholera toxin interacted with NAD using the Docking method. As a result of interaction analysis, the 12 amino acid region (called 61- STSISLRS AHLV-72) binding NAD were detected (Figure 5), and energy calculations of the region were made (figure 6) (Table 1).

Table 1: Energy calculations of binding region of CT

	$\Delta G$ (coulomb)	$\Delta G$ (vdw)	$\Delta G$ (covalent)	$\Delta G$ bind
Cholera Toxin	-16,822	-36,678	9,169	-47,392

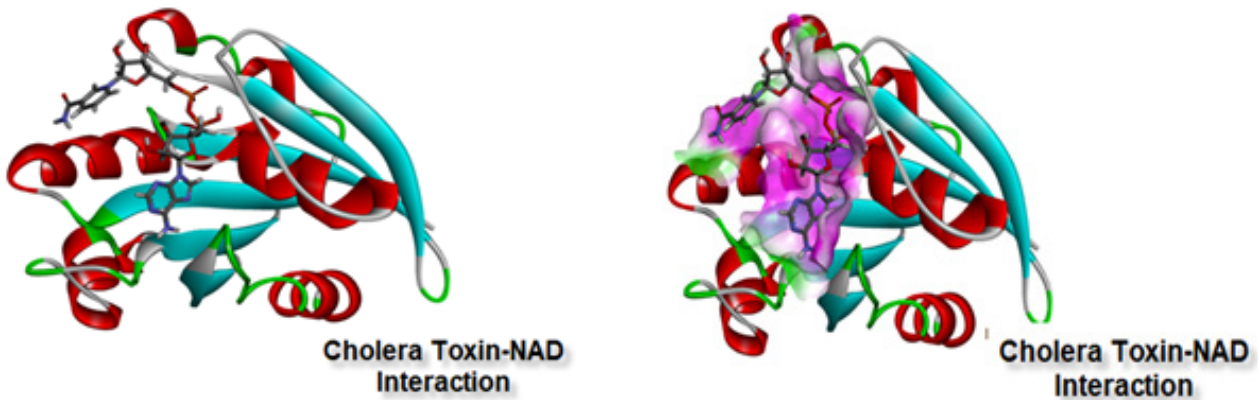


Figure 5: Interaction Area of Cholera Toxin with NAD.

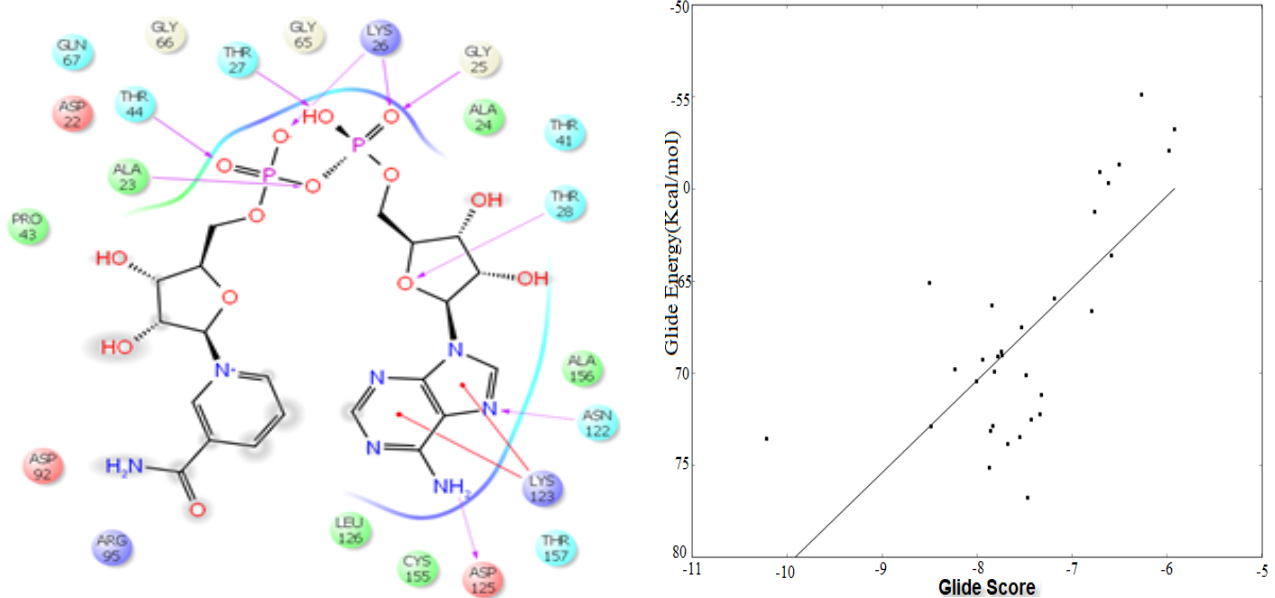


Figure 6: Interaction residue and energy calculations of Cholera Toxin with NAD.

In order to analyze binding interactions between cholera toxin and NAD<sup>+</sup>, molecular dynamics (MD) simulations and the CHARMM algorithm at 300 °K mean temperature and under pH 7 were used. Also, to find the flexibility of cholera toxin and the most probable conformation which it can be found in, the NAMD algorithm was used; and besides the studies are still ongoing down to the nano-second range. Protein docking studies were performed using the autodock program. In the studies the calculations were made using a fixed protein docking program based on the Fast Fourier Transform (FFT) correlation approach, and they were extended to use the potentials for double logical interaction.

By adding Diphtheria Toxin (1TOX), Cholera Toxin (2A5F), Iota Toxin (1GIQ), vip2 (1QS2) and Cholix Toxin (2Q6M) from ADPRT groups to our study, the structures of these extracellularly produced toxins were investigated in molecular dynamics methods. Before the studied ADPRTs are interacted with NAD in the most ideal conditions in the computer environment by using the AutoDock program, the process of preparing a series of data sets was started. In the study receptor grids were created for ADPRTs by using PDB (Protein Data Bank) files. In the next step the ligand chemical structure for NAD was prepared using the AutoDock program. The similarity (RMSD) calculations of representatives of both groups were extracted (Table 2).

Table 2: Comparative RMSD Values (Å) of ADPRT groups

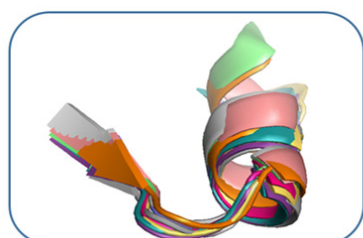
RMSD (Å)	Diphtheria Toxin	Cholera Toxin	lota toxin	Vip2	Cholix
Diphtheria Toxin	0,00	4.14	4.40	4.12	3.17
Cholera Toxin	4.14	0,00	3.93	5.45	4.50
lota toxin	4.40	3.93	0	2.63	4.50
Vip2	4.12	5.45	2.63	0,00	3.90
Cholix	3.17	4.50	4.50	3.90	0,00

After the prepared data sets, in order to determine the interaction sites of the common motif that recognizes NAD, so that ADPRTs can catalyze NAD, the necessary docking was done to determine the binding energy required for the interaction interface of this common motif to bind to the NAD region. As a result of the docking process, the binding energies were calculated in order to determine the interaction regions with the highest probability of binding by using the Glide XP scoring technique (Table 3).

Table 3: Free Energy Binding Calculations of ADPRTs with NAD

	$\Delta G$ (coulomb)	$\Delta G$ (vdw)	$\Delta G$ (covalent)	$\Delta G$ bind
Cholera Toxin	-16,822	-36,678	9,169	-47,392
lota-Toxin	-43,382	-57,098	12,396	-62,209
VIP2	-12,039	-57,08	10,319	-65,618
Diphtheria Toxin	-59,308	-50,099	-2,541	-92,407

Then, the motifs formed by the toxin groups and recognizing and catalyzing NAD were overlapped and the structural similarities were examined, and the common structural model was displayed (Figure 7).



```

TOX_B YSTDNKYDAAGM SVDNENELSGKAGGVVRYTFGLTKVLALKVD
ASF_B STSLRSALHY--GOTILSGHSTYIIYVIYIATAENMENVNDVLGA
GIQ_A STSLGSVNMSAFARRKIILRLINIPKDSBGAVLSAIBGVAGEYEVL
QS2_A STSLSSERLAAPSSRKIILRLQVPRGSGAYLSAIGGFASEKEIL
Q6M_A YVATHAEVAHG YARIKEGTGEYGLETRAERDARGVMILRVYIPRAS

```

Figure 7: Comparison of Toxin Groups

As a result of the analysis on toxin groups, it was found that the region of approximately 12 acids, starting with Y (Tyrosine) and ending with Y or starting with STS (Serine-Threonine-Serine) amino acids, is on the active site (Figure 8 and 9). In addition it was concluded that a common motif which may occur in this region may be the region that binds to NAD.

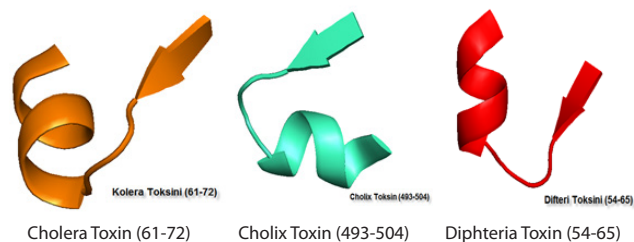


Figure 8: Active sites recognizing NAD, which start with Y amino acid and also end with Y amino acid belonging to the ADPRT group.

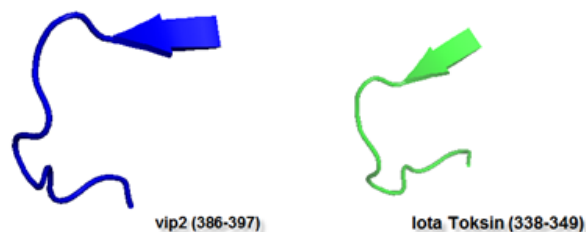
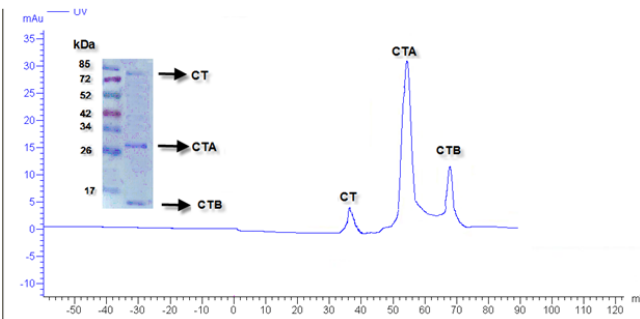


Figure 9: Active sites recognizing NAD, which start with the STS amino acid sequence belonging to the ADPRT group.

At the end of the study, the regions most likely to interact with NAD from the ADPRT groups and the amino acid sequences belonging to these regions were determined to be used in future theoretical and experimental studies (Table 4). As a result of the study, it was theoretically determined that the regions of STS (Ser-Trp-Ser)-10/12 amino acids (starting with Serine-Tryptophan-Serine and taking 10 amino acids) have a structural conformation that recognizes NAD.

Table 4: Regions most likely to interact with NAD from ADPRT groups				
PDB_Id	Resolution (Å)	ADPRT	Length	ADPRT - INTERACTION SERIES
2A5F	2.02	Kolera Toksini	12	<sup>61</sup> -STISILRSAHLV- <sup>72</sup>
1GIQ	1.80	Ioto Toksin	12	<sup>336</sup> -STSIGSVNMSAF- <sup>347</sup>
1QS2	2.70	VIP2	12	<sup>386</sup> -STSLSSERLAAF- <sup>392</sup>
1TOX	2.30	Difteri Toksini	12	<sup>54</sup> -YSTDNKYDAAGY- <sup>65</sup>

In order to examine the information which was obtained theoretically in our study, an experimental study was carried out on commercially available cholera toxin (sigma-C8052). The sample, which was confirmed to be cholera toxin by electrophoretic processes, was partially digested with trypsin, and then it was separated into fragments by passing through a spherical s-100 column to be cut (Figure 10).



**Figure 10: Decomposition of cholera toxin into fragments. A. (1) Protein weight marker, (2) After toxin clipping, was eluted in (10 µg) SDS/PAGE. B. Cholera toxin (0.2 mg), which was partially digested with trypsin as described in the methods, was separated in sephacryl S-100 chromatography. Flow rate 0.8 ml/min, sample volume 0.5 ml. Measurement A280 nm.**

The toxicity of the CTA part of the cholera toxin was determined on the HUVEC cells (Figure 11). CTA was tested by thermal shift assay, which is a protein-ligand interaction method. Fluorescent-based thermal shift experiment was carried out as mentioned in the materials and methods. The interaction of the cholera toxin fragment CTA-NAD was examined. For each NAD concentration, a denaturation curve was created in the RT-PCR device by increasing the temperature, and melting degrees ( $T_m$ ) were calculated. The thermal stability of CTA was found to increase when interacting with NAD (Figure 12). Based on the thermal stability graphs measured from the linear region after the CTA-NAD interaction,  $T_m$  values were calculated from the Boltzman equation with GraphPad and Excel (Figure 13).

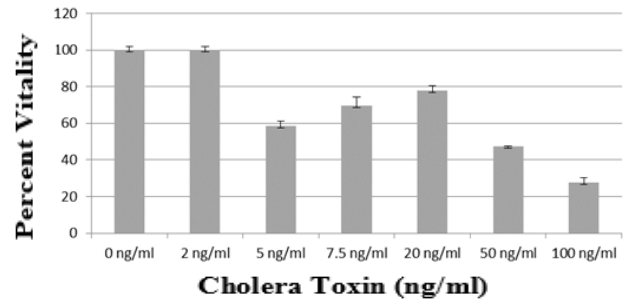


**Figure 11: Cholera Toxin 24 hour % viability test. Viability was measured with MTT.**

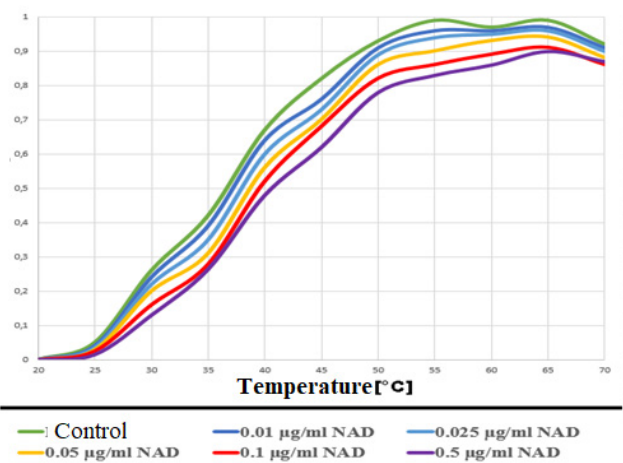


**Figure 12: The interaction of cholera toxin CTA-NAD was tested by thermal shift assay. After the application of 10 µg/ml CTA1 and increasing concentrations of NAD in the presence of SYPRO Orange, the fluorescent intensity was measured at a wavelength of 580 nm for 10 seconds (0.5 °C/15 sec) at 0.5 °C between 20 °C and 90 °C. Nad was not applied in the control.**



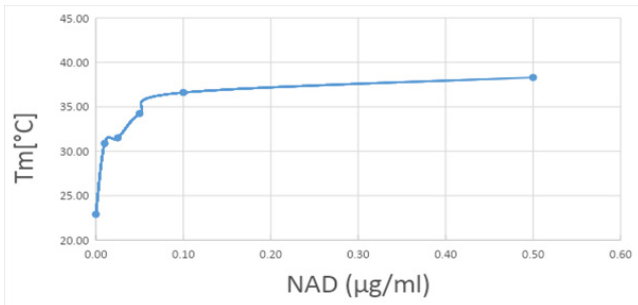


**Figure 13: After the CTA-NAD interaction, T<sub>m</sub> values from the measured thermal stability graphs were calculated with GraphPad and Excel. In the table, the semi-denaturing temperature (T<sub>m</sub>) values obtained by calculating from the linear region were calculated by using the Boltzman equation.**

*Vibrio Cholerae* secrete Cholera Toxin and also CT is carried extracellularly by the system which is called the type II secretion system. This system contains more than a dozen interacting proteins and it ensures that toxin and other proteins such as extracellular enzymes are exported from the periplasm through the outer membrane (17). The signification of CT is regulated by several transcriptional activators controlled by the *V. cholerae* "quorum-sensing system" (18). Whereas the expression of CT increases at low cell densities, the quorum-sensing system downregulates CT synthesis at high cell densities. The key step for intoxication is the entry of CTA into the cell cytosol because the ADP-ribosylation of the trimeric G<sub>s</sub> component of AC is catalyzed by CTA. The ADP-ribosylation factors (ARFs) known as a family of essential and ubiquitous G proteins activate this enzymatic reaction allosterically. The crystal structures of a CTA/ARF6-GTP complex show that the binding of ARF activator causes remarkable changes in CTA loop regions which enable the nicotinamide adenine dinucleotide (NAD<sup>+</sup>) substrate to bind to the active site (19). ADPRT is a better defined toxin group than other toxin groups in terms of both its structure and effect. In particular diphtheria toxin from this group is divided into two parts after limited proteolytic digestion. The toxin consists of fragment A (FA) with enzymatic function (ADP-ribosyltransferase), corresponding to its N-terminal point, and fragment B (FB), which allows holotoxin to bind to the cell (20). The enzymatic part (FA) of the toxin reaches the cytoplasm in the endocytic process. FA entering the cell causes inhibition of protein synthesis, DNA splicing, destruction of the actin skeleton, and apoptosis (21). CT group toxins are the structures that cause apoptosis or necrosis in the cells which they have affected by targeting various essential proteins in host organisms. Although ADPRT

enzymes display a different diversity of functions and low sequence identities, they share common structural and functional features. Firstly, they catalyze a common reaction, namely ADP-ribosylation. Secondly, they have structurally similar catalytic sites that bind NAD<sup>+</sup>. In our study we investigated the common NAD binding motifs of CT, a member of the ADPRT family, which also occurs in other members of the family. At the end of our study, as stated in the findings, we found a region of 12 amino acids. We classified this region into two groups. These are the regions starting with Y- [10 amino acids] – Y tyrosine and ending with tyrosine in the first group, and the sequences starting with STS- [9 amino acids] Serine-Threonine-Serine in the second group. Although the sequences of non-common amino acids of these regions vary, we believe that their three-dimensional structures are similar and that these common regions are important in the recognition and catalysis of NAD. Our experimental studies showing the parts containing the catalytic regions determined as a result of the theoretical studies also confirm these results. In the context of protein-protein, protein-ligand interactions, the affinity constants of ADP-ribosylating toxins (diphtheria and cholera) with NAD are known. We demonstrated this interaction for the first time with thermal shift assay (TSA) studies, which have found significant use in recent years. After ligand binding to native protein, the resistance to thermal effects increases. T<sub>m</sub> values from the denaturation curves after NAD binding were determined according to the Boltzman equation. As the affinity of the ligand to the protein increases, the denaturation temperature increases. By using this method we experimentally observed that the amount of CT binding also increased, with the increasing concentration of CT. Our work was supported by TUBITAK as project number 113S334.

## CONCLUSION

In this study an important member of the ADPRT family and CT was simulated using docking software. In consequence of theoretical analyses, we provided an insight into the interaction of the structure with NAD by anticipating the binding of this enzyme to NAD and determining that it has a common structural pattern with DT and CT enzyme groups. CT binds to NAD with 12 amino acids called 61- STSISLRS AHLV-72. That was verified experimentally. Our data showed that the three-dimensional structures of CT and ADPRT are similar although their sequences vary widely. The interaction mechanisms and protein structures of CT and DT shared similarity in catalytic domains whereas they showed differences in substrate proteins.

## REFERENCES

1. Bentivoglio M., Pacini P. (1995). Filippo Pacini: a determined observer. *Brain research bulletin*, 38(2), 161–165.
2. Chaudhuri K., Chatterjee S.N. (2009). *Cholera toxins*. Springer Science & Business Media.
3. De S.N. (1959). Enterotoxicity of bacteria-free culture-filtrate of *Vibrio cholerae*. *Nature*, 183(4674), 1533–1534.
4. Dutta N.K., Panse M.V., Kulkarni D.R. (1959). Role of cholera toxin in experimental cholera. *Journal of bacteriology*, 78(4), 594–595.
5. Finkelstein R.A., LoSpalluto J.J. (1969). Pathogenesis of experimental cholera. Preparation and isolation of cholera toxin and cholera toxinogen. *The Journal of experimental medicine*, 130(1), 185–202.
6. Finkelstein R.A., LoSpalluto J.J. (1970). Production of highly purified cholera toxin and cholera toxinogen. *The Journal of infectious diseases*, 121, 63+.
7. Zhang R.G., Scott D.L., Westbrook M.L. et al. (1995). The three-dimensional crystal structure of cholera toxin. *Journal of molecular biology*, 251(4), 563–573.
8. Sigler P.B., Dryan M.E., Kiuefer H.C., Finkelstein R.A. (1977). Cholera toxin crystals suitable for x-ray diffraction. *Science (New York, N.Y.)*, 197(4310), 1277–1279.
9. Finkelstein R.A., Boesman M., Neoh S.H., LaRue M.K., Delaney R. (1974). Dissociation and recombination of the subunits of the cholera enterotoxin (cholera toxin). *Journal of immunology (Baltimore, Md. : 1950)*, 113(1), 145–150.
10. Beddoe T., Paton A.W., Le Nours J., Rossjohn J., Paton J.C. (2010). Structure, biological functions and applications of the AB5 toxins. *Trends in biochemical sciences*, 35(7), 411–418.
11. Wang H., Paton J.C., Herdman B.P. et al. (2013). The B subunit of an AB5 toxin produced by *Salmonella enterica* serovar Typhi up-regulates chemokines, cytokines, and adhesion molecules in human macrophage, colonic epithelial, and brain microvascular endothelial cell lines. *Infection and immunity*, 81(3), 673–683.
12. Vanden Broeck D., Horvath C., De Wolf M.J. (2007). *Vibrio cholerae*: cholera toxin. *The international journal of biochemistry & cell biology*, 39(10), 1771–1775.
13. Baldauf K.J., Royal J.M., Hamorsky K.T., Matoba N. (2015). Cholera toxin B: one subunit with many pharmaceutical applications. *Toxins*, 7(3), 974–996.
14. Odumosu O., Nicholas D., Payne K., Langridge W. (2011). Cholera toxin B subunit linked to glutamic acid decarboxylase suppresses dendritic cell maturation and function. *Vaccine*, 29(46), 8451–8458.
15. Cornell W.D., Cieplak P., Bayly C.I. et al. (1995). A second generation force field for the simulation of proteins, nucleic acids, and organic molecules. *J Am Chem Soc* 117: 5179– 5197.
16. Brunelle J.L., Green R. (2014). One-dimensional SDS-polyacrylamide gel electrophoresis (1D SDS-PAGE). *Methods in enzymology*, 541, 151–159.
17. Johnson T.L., Abendroth J., Hol W.G., Sandkvist M. (2006). Type II secretion: from structure to function. *FEMS microbiology letters*, 255(2), 175–186.
18. Lin W., Kovacicova G., Skorupski K. (2007). The quorum sensing regulator HapR downregulates the expression of the virulence gene transcription factor AphA in *Vibrio cholerae* by antagonizing Lrp- and VpsR-mediated activation. *Molecular microbiology*, 64(4), 953–967.
19. O'Neal C.J., Jobling M.G., Holmes R.K., Hol W.G. (2005). Structural basis for the activation of cholera toxin by human ARF6-GTP. *Science (New York, N.Y.)*, 309(5737), 1093–1096.
20. Unlü A., Bektaş M., Sener S., Nurten R. (2013). The interaction between actin and FA fragment of diphtheria toxin. *Molecular biology reports*, 40(4), 3135–3145.
21. Bektaş M., Varol B., Nurten R., Bermek E. (2009). Interaction of diphtheria toxin (fragment A) with actin. *Cell biochemistry and function*, 27(7), 430–439.